RESEARCH ARTICLE

VOLCANICA

An appraisal of the observed crystallinities of volcanic materials

Hannah I. Shamloo*[α] and Adam J. R. Kent[β]

[α] Department of Geological Sciences, Central Washington University, Ellensburg, WA, 98926 USA.
[β] College of Earth, Ocean, and Atmospheric Sciences, Oregon State University, Corvallis, OR 97331 USA.

Submitted: 2023-07-07 | Accepted: 2024-01-09 | Published: 2024-02-22

Editor: J. Vasseur | Typesetter: J. Farquharson

Abstract

There is a broad consensus that magma eruptibility—the ability of magma stored in the subsurface to erupt onto Earth's surface—is strongly controlled by viscosity. Related to this, a critical parameter that controls viscosity is crystallinity. However, there is uncertainty in the crystallinities that distinguish eruptible from non-eruptible magmas, and whether highly crystalline magmas (>60 vol.%) could be erupted in some conditions. An underutilized but important source of information for understanding this relationship is the observed crystallinities in erupted volcanic materials, which by definition represent a set of eruptible magmas. Here we present a compilation of reported crystallinities for nearly 1000 volcanic samples of differing composition, tectonic setting, and eruption style, which provides valuable insight into the fundamental mechanisms which drive eruptions. Overall, the 95th percentile crystallinity value of our full dataset is 57 vol.%, and >99 % of all non-dome samples have crystallinity ≤53 vol.%. This suggests that 50–60 vol.% crystallinity represents a fundamental limit for eruptibility for most volcanic rocks. Some dome samples are clear exceptions to this and are erupted with considerably higher crystallinities. There is also a significant correlation between crystallinity and whole rock SiO_2 content as observed previously, but a shallow slope suggests whole rock and melt silica content have less impact on critical crystallinity for erupted magma than previously thought. Melt viscosity (as a function of SiO_2, temperature, and H_2O content) and crystallinity both play important roles on increasing effective viscosity, where melt viscosity plays a more important role at low crystal fractions, and crystallinity plays a more important role at crystallinities greater than ~40 vol.%.

Non-technical summary

The proportion of solid crystals to liquid melt in a magma influences its ability to flow and erupt, analogous to drinking a slushy mixture (i.e. solid ice and liquid juice), where a mostly frozen slushy mixture is difficult to drink through a straw (i.e. a crystal-dominated magma that is difficult to erupt) compared to a melted slushy mixture easy to drink through a straw (i.e. a melt-dominated magma that is easily erupted). However, the exact ratio of crystals to melt for a magma that can be erupted versus one that cannot remain uncertain. This study provides a compilation of crystal contents for volcanic rocks from a range of settings and magma compositions. Most erupted magmas have crystallinities <60 vol. % crystals, providing insight into the threshold between eruptible and non-eruptible magmas.

Keywords: Eruptibility; Magma viscosity; Magma crystallinity; Critical crystallinity.

1 Introduction

Volcanic eruptions, by definition, require the movement of magma from Earth's interior to the surface. There is wide consensus that the ability of a given magma to ascend through the crust and erupt (i.e. eruptibility) is strongly controlled by its viscosity [e.g. Marsh 1981; Rubin 1995; Scaillet et al. 1998]. As a result, viscosity is one of the most important properties in understanding the likelihood of a magma to erupt and can also have a major influence on the resulting eruption style [e.g. Jaupart and Allègre 1991; Dingwell 1996; Papale 1999; Gonnermann and Manga 2003; Ruprecht and Bachmann 2010; Koleszar et al. 2012; Okumura et al. 2019]. Therefore, understanding the pre-eruptive viscosity of an erupted magma has the potential to assist in forecasting the timing and style of future volcanic events.

A variety of factors control magma viscosity including temperature, composition of the silicate liquid component, the structure of the silicate liquid, as well as the proportions, size distributions, and shapes of bubbles and crystals present [e.g. Marsh 1981; Mysen and Neuville 1995; Neuville and Mysen 1996; Giordano et al. 2008; Mader et al. 2013]. As magma cools, it becomes more viscous, reflecting both the increased polymerization of the silicate liquid at lower temperatures, and an increased crystal fraction as crystals form from cooling magma [e.g. Neuville and Mysen 1996; Giordano et al. 2008; Takeuchi 2011]. Thus, the thermal evolution of magma is also closely tied to viscosity, and the abundance of crystals is an important control on viscosity, particularly at temperatures that approach the solidus [e.g. Marsh 1981; Lejeune and Richet 1995; Caricchi et al. 2007; Ishibashi and Sato 2007; Cooper and Kent 2014]. Bubbles can also act to make magma either more or less viscous, depending on their deformability [e.g. Takeuchi 2011; Mader et al. 2013], but this effect is often relatively minor relative to crystallinity [Scaillet et al. 1998]. It should also be noted that the shape of the particles, their orientation, and particle-particle interaction also play a role in the rheological response of crystal-bearing melts, however these effects are not explored in this study [Manga et al. 1998; Mueller et al. 2010; Cimarelli et al. 2011; Mueller et al. 2011; Pereira et al. 2022; Pereira Machado et al. 2022].

Although there is wide consensus regarding the important relationship between crystallinity, viscosity, and eruptibility [e.g. Popa et al. 2021; Okumura et al. 2022], there is

* shamlooh@cwu.edu

also increasing recognition of the complexity of this relationship. Past studies discuss a critical transition for a cooling and crystallizing magma in which crystallinity increases until viscosity is dominated by crystal-crystal interactions, and the magma effectively behaves like a solid [Marsh 1981]. At this point, magmas reach rheological "lock-up", and are unable to flow along fractures, and therefore are considered to be non-eruptible [Marsh 1981]. Typically, this critical crystallinity is accepted to be around 40–60 vol.% crystals (avg. 50 vol.%), equivalent broadly to viscosities of 10^6–10^{12} Pa.s [e.g. Marsh 1981; Brophy 1991; Scaillet et al. 1998; Bachmann 2004; Hildreth 2004; Takeuchi 2011; Solano et al. 2012]. However, more recently, the idea of a single critical crystallinity value has received more scrutiny, and there is broad agreement that a specific "lock-up" point is also dependent on a range of factors such as crystal type and shape, liquid composition, and strain rate [Caricchi et al. 2007; Bergantz et al. 2017]. This discussion is also made more relevant by the wide recognition that magma stored within the crust is in a crystal-rich "mushy" state [e.g. Bachmann and Bergantz 2008; Cooper and Kent 2014; Klemetti and Clynne 2014] or even subsolidus [e.g. Mucek et al. 2021; van Zalinge et al. 2022]. Thus, the crystallinity at which magmatic mushes can be remobilized and/or erupted is also of importance, but also uncertain. Note, there may also be differences in mobilization or disruption of a magma mush versus eruption of a magma mush, as these processes are not necessarily coupled and could happen at different viscosities [Bergantz et al. 2017]. For the purpose of this study, we focus on the eruption of crystal-bearing magmas, rather than remobilization or disruption.

There is also suggestion that magma may be erupted at crystallinities that exceed 50–60 vol.%. For example, recent experiments suggest magma mushes with high crystallinities can be erupted explosively due to the feedback between decompression rates and retention of bubbles, where fast decompression rates cause bubble retention to disrupt the crystal framework and reduce viscosity of a magma mush with crystallinity as high as >70 vol.%. This substantial reduction in magma viscosity provides potential for remobilization and even eruption [Pistone et al. 2017; Okumura et al. 2021]. Extrusion of highly crystalline or even subsolidus material in lava domes has also been suggested [e.g. Pistone et al. 2017; Mucek et al. 2021]. There is notable effort currently going into gaining greater understanding of these processes via numerical and experimental studies [e.g. Bergantz et al. 2017].

Although valuable insights into the viscosity of silicate magmas come from experimental, theoretical, and numerical studies, an important but less recently utilized source of information in these investigations is the observed crystallinities in volcanic material erupted across different terrestrial settings, for magmas of different compositions, and by different eruption styles. Earlier compilations of crystallinity values were influential. For example, the seminal work of Marsh [1981] led to the widespread use of ~50 vol.% crystals as the critical volume of crystals at which it becomes impossible to erupt crystal-bearing magma. However, the Marsh [1981] compilation was also based on a relatively small number (n = 60) of lavas and other samples specifically from the Aleutian arc. Further efforts have expanded the number of samples and eruption styles but have also been relatively restricted in size and scope, and often focused on specific magma compositions or eruption styles [Ewart 1976; Brophy 1991; Scaillet et al. 1998; Takeuchi 2011]. To provide greater empirical constraints on the crystallinity of eruptible magmas we present herein a comprehensive compilation of 950 reported crystallinities of volcanic rocks from a range of references. Our compilation includes a variety of magma compositions, eruption styles, and tectonic settings and represents a fundamental dataset for future efforts to evaluate the effect of crystallinity on magma eruptibility.

2 Methods: Data compilation and calculations

The crystallinities of erupted material, expressed as volume percent, were compiled from the literature along with tectonic setting, eruption style, and when available, whole rock and glass major element chemistry. Different techniques were used to determine crystallinity including tomography, modal point counts and visual estimates, or in some cases were not specified in the study. We acknowledge here that the method for determining crystallinity matters, where the most quantitative means of determining crystallinity is by 2D or 3D analysis (e.g. X-ray diffraction, microtomography, or image analysis), and the least quantitative is by visual estimate. In most scenarios, the method of determining crystallinity was not specified in the various studies used for this compilation, therefore our hope is that future work can build on our dataset and quantify the variation between methodology.

Our dataset includes samples from past compilations [Marsh 1981; Brophy 1991; Scaillet et al. 1998; Takeuchi 2011] as well as many other references (~200) compiled for this study (Supplementary Material*, Figure S1). The range of bulk compositions compiled is 45–80 wt.% SiO_2, and eruptive styles have been categorized into four groups by their deposit type, including lava, lava dome (referred to as just "dome" in this study), tephra, and ignimbrite. Note the Brophy [1991] dataset is from individual lava or domes from orogenic volcanic centers, but the sample type is not specifically reported for each analysis. Thus, where we need to separate these eruption styles, we do not use the Brophy [1991] dataset. Each sample was also categorized by tectonic setting either as subduction, rift zone, and intraplate, following the classification of Global Volcanism Program†.

For past compilations where data tables were unavailable, the data was manually digitized using `Web Plot Digitizer` [Rohatgi 2014], and consequently some of the data from these studies is incomplete. In addition, because the source data for past compilations is unidentified, it is possible that there are some repeat data in our compilation. For the additional studies compiled here (excluding past compilations data), crystallinity was often reported as a range for a given sample suite, and therefore the midpoint between a minimum and maximum is used. In other cases, an individual crystallinity was reported per sample, which is then reported as a single value. We acknowledge there are additional sources in the literature that

*https://zenodo.org/deposit/7754305
†https://volcano.si.edu/

report crystallinities that we have missed and invite others to build upon our freely available dataset.

Liquid viscosity calculations were performed following Giordano et al. [2008] for every sample that had recorded major element chemistry of coexisting glass (n = 124). Note, the majority of samples are subalkaline, which are better suited for this model (Supplementary Material, Figure S2). Temperature for each liquid calculation was assigned discretely based on SiO_2 content. For example, for compositions where SiO_2 is 45–50 wt.%, a discrete temperature of 1200 °C was assigned. For 50–55 wt.% SiO_2: 1100 °C; 55–60 wt.% SiO_2: 1000 °C; 60–65 wt.% SiO_2: 900 °C; 65–70 SiO_2: 850 °C; 70–75 SiO_2: 800 °C; 75–80 SiO_2: 750 °C. Water content is less straight-forward and will vary with a given magma SiO_2 content, pressure, and extent of saturation. Therefore, liquid viscosities were calculated for a range of water contents including 0.5, 2.0, and 5.0 wt.% H_2O.

Calculated liquid viscosities for each glass sample were then used to determine suspension viscosities for crystal-liquid mixtures using the Maron and Pierce [1956] approach:

$$\eta_r = \frac{\eta_s}{\eta_m} = \left(1 - \frac{\phi}{\phi_m}\right)^{-2.0} \quad (1)$$

where η_r is relative viscosity, η_s is the viscosity of the crystal-liquid suspension or mixture, also known as "suspension viscosity", η_m is the viscosity of the melt portion only, ϕ is the volume fraction of crystals, and ϕ_m is the maximum packing fraction, or the volume fraction beyond which there is no space remaining to accommodate further particles in a material. This value is based on the geometry and dispersal of crystal particles [Mader et al. 2013]. Note, a similar approach exists that utilizes a modified version of the Einstein-Roscoe equation with 2.5 as the exponent value instead of 2.0 used here [Roscoe 1952; Sato 2005; Ishibashi and Sato 2007]. However, it has been demonstrated that the exponent value of 2.0 better describes suspension viscosity data as a function of particle volume fraction [Sato 2005; Ishibashi and Sato 2007], therefore we use the Maron and Pierce [1956] relationship.

Equation 1 is rearranged to solve for suspension viscosity, sometimes referred to as "effective viscosity" [e.g. Einstein 1906; Roscoe 1952; Stevenson et al. 2001; Giordano et al. 2008; Vetere et al. 2010] which describes magma viscosity with the consideration of the presence of crystals:

$$\eta_s = \eta_m * \left(1 - \frac{\phi}{\phi_m}\right)^{-2.0} \quad (2)$$

The maximum packing fraction values (ϕ_m) are a function of the aspect ratio of the suspended particles (see values reported in Ishibashi and Sato [2007] and Mueller et al. [2011]). Despite the variety of crystal shapes in natural silicates, we use a single ϕ_m value of 0.6, determined empirically by Marsh [1981], which is commonly used for random close packing of monodisperse spheres or oblate crystals [Maron and Pierce 1956; Mueller et al. 2010].

3 Results

Of the 950 samples compiled in this study, the recorded crystallinities range from <1 vol.%, a maximum of >99 vol.%, a median of 31 vol.%, and a mode of 10 vol.% (Figure 1A). Most of the dataset falls within 2 to 55 vol.% crystals (5th and 95th percentile; Figure 1B). There is a sharp drop off in the distribution at ~60 vol.% crystals, although a smaller number of samples, all coming from lava domes, have crystallinities up to >99 vol.% (Figure 2). All histogram figures use Sturges rule to determine bin size, where the number of bins is approximated by $\log_2(n) + 1$ as a guide. Note we apply small variations to this rule to maintain consistency within individual figures. A kernel density estimate (kde) was calculated for each dataset to ensure that the choice of bin size did not distort the distribution, and is shown with each histogram as a solid line.

Figure 2 shows samples grouped by eruption style, such as lava, dome, tephra, and ignimbrite samples. Due to the Brophy [1991] compilation not explicitly reporting whether a sample was a lava or lava dome, their compilation was excluded here, but can be seen included in Supplementary Material, Figure S3. Without the Brophy [1991] compilation, the median crystallinities for lava, dome, tephra, and ignimbrites are 27, 42, 28, and 13 vol.% (Figure 2A; Table 1). Maximum recorded crystallinities for lava, tephra, and ignimbrite samples are 61, 57, and 58 vol.%, whereas the maximum recorded crystallinity for lava domes is >99 vol.%. The 5th and 95th percentile values for the distributions for lava, dome, tephra, and ignimbrites are 1 and 50 vol.%, 16 and 78 vol.%, 4 and 53 vol.%, and 3 and 51 vol.%. Thus, only dome eruptions show an appreciable proportion of erupted magmas with crystallinities greater than 60 vol.%. Cumulative distribution functions (CDF) further illustrate the distribution of crystallinities within each sample set (Figure 2B). Lava and tephra CDFs are very similar, showing a relatively even distribution of crystallinities between 0–60 vol.%. Ignimbrite and dome CDFs diverge from lava and tephra CDFs, where ignimbrite samples have a higher frequency of samples with lower crystallinities (i.e. between 0–20 vol.%) and dome samples have a higher frequency of samples with higher crystallinities (i.e. between 30–80 vol.%). Crystallinities grouped by tectonic setting such as subduction zone, rift zone, and intraplate, show 95th percentile values of 58, 38, and 20 vol.% crystals (Table 1); however a greater number of rift zone and intraplate samples is required to confirm this observation, as they are under sampled in this compilation (Supplementary Material, Figure S5).

Crystallinities for samples with reported SiO_2 contents (n = 884, including the Brophy [1991] dataset) are summarized in Figures 3 and 4. In general, there is a significant correlation between whole rock SiO_2 content and crystallinity based on P value, where a low P value (~0.05) represents a low probability of the calculated R value being generated from a random dataset of this size (solid line labelled "full dataset" Figure 3A; Table 1). When data is binned and the maximum crystallinity value is calculated for each bin and used to plot a linear regression with SiO_2 content, we observe a weak correlation (P = 0.29). However, the slope of this linear regression (dot-dash line labelled "max. crystallinity" Figure 3A; Table 1) is similar to the slope of the linear regression for the overall dataset (solid line, "full dataset" Figure 3A). Note that we do not include dome samples with intermediate compositions and very high crystallinities when we consider maximum val-

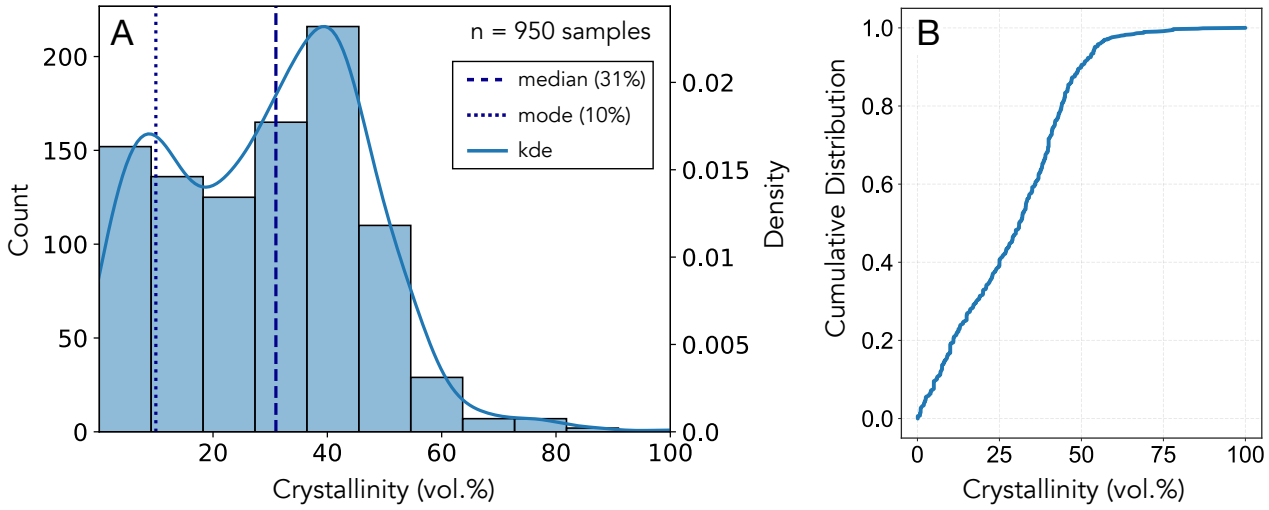

Figure 1: [A] Compilation of reported crystallinities from 950 samples compiled from the literature. The minimum and maximum crystallinity recorded is <1 vol.% and 99 vol.%, a median of 31 vol.% (dashed vertical line), and a mode of 10 vol.% (dotted vertical line). A bin size of 11 was chosen based on Sturges rule. A kernel density estimation (kde) is shown by the solid line and has an associated y-axis labelled "Density". [B] Cumulative distribution of all recorded crystallinities. Note the 5th and 95th percentile for the cumulative distribution is 2 to 55 vol.% crystals.

Table 1: Statistical values for datasets with known SiO_2 contents, including linear regression between crystallinity and SiO_2 content, and the 5th and 95th percentile values for a given cumulative distribution. Datasets exclude Brophy [1991] compilation unless otherwise noted. Figures S4 and S5 can be found in Supplementary Material.

Sample type	*n*	5th (vol.% xtals)	95th (vol.% xtals)	Slope $\left(\frac{\text{vol.\% xtals}}{\text{wt.\% SiO}_2}\right)$	Slope Std. Err.	R	R^2	p value
Marsh [1981] Lavas (Figure 3 dash line)	41	3	49	−4.1	0.34	0.84	0.7	<0.05
Whole rock† (Figure 3A solid line)	760	2	55	−0.68	0.07	−0.33	0.11	<0.05
Whole rock max† (Figure 3A dot-dash line)	760	2	55	−0.6	0.52	−0.38	0.14	0.29
Glass (Figure 3B solid line)	124	3	51	0.42	0.19	0.2	0.039	0.03
Glass max (Figure 3B dot-dash line)	124	3	51	1.1	0.31	0.77	0.6	0.009
Lava (Figure 2 & S4)	105	1	50	−0.74	0.12	−0.52	0.27	<0.05
Dome (Figure 2 & S4)	46	16	78	−1.7	0.5	−0.45	0.21	0.002
Tephra (Figure 2 & S4)	177	4	53	0.007	0.17	0.003	0.000 011	0.97
Ignimbrite (Figure 2 & S4)	48	3	51	−0.11	0.51	−0.033	0.0011	0.82
Subduction Zone† (Figure S5)	808	4	55	−0.32	0.068	−0.16	0.026	<0.05
Rift Zone (Figure S5)	68	0.1	38	0.038	0.27	0.017	0.0003	0.9
Intraplate Zone (Figure S5)	8	7	20	−0.13	0.34	−0.15	0.02	0.7

† Dataset includes Brophy [1991] compilation.

ues for each bin. In addition, we observe that crystallinity and SiO_2 content show a significant correlation when grouped by lavas, but not for dome, tephra, or ignimbrite, although the sample size of dome, tephra, and ignimbrite datasets are smaller than that of the lava dataset (Table 1; Supplementary Material, Figure S4). When grouping data by tectonic setting (i.e. subduction zone, rift zone, intraplate), there is no correlation between SiO_2 content and crystallinity, although there is also room for improvement with this observation considering the uneven sampling between tectonic settings as stated prior (Table 1; Supplementary Material, Figure S5). Lastly, when grouping the data by glass composition, there is no significant correlation, although the dataset is much smaller in size (solid line labelled "full dataset" Figure 3B; Table 1).

Of the dataset where all major elements were available as glass analyses (n = 124), effective viscosities (i.e. viscosity of a melt-crystal mixture, or "suspension viscosity") were calculated for a range of temperatures and water contents

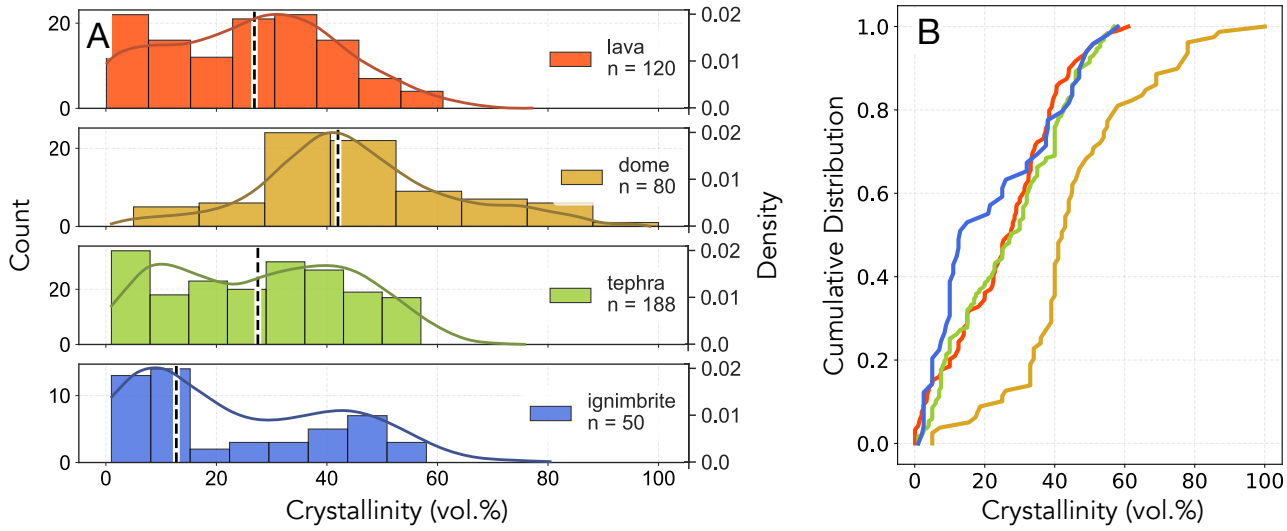

Figure 2: [A] The distribution of crystallinities grouped by eruptive style/sample type *excluding* the Brophy [1991] compilation (bin size = 8; see text). A kernel density estimate is also included for each panel. The dashed vertical line marks the median crystallinity of each distribution. [B] Cumulative distribution functions (CDF) of each eruptive style. The 5th and 95th percentile values for the distributions for lava, dome, tephra, and ignimbrites are 1 and 50 vol.%, 16 and 78 vol.%, 4 and 53 vol.%, and 3 and 51 vol.%.

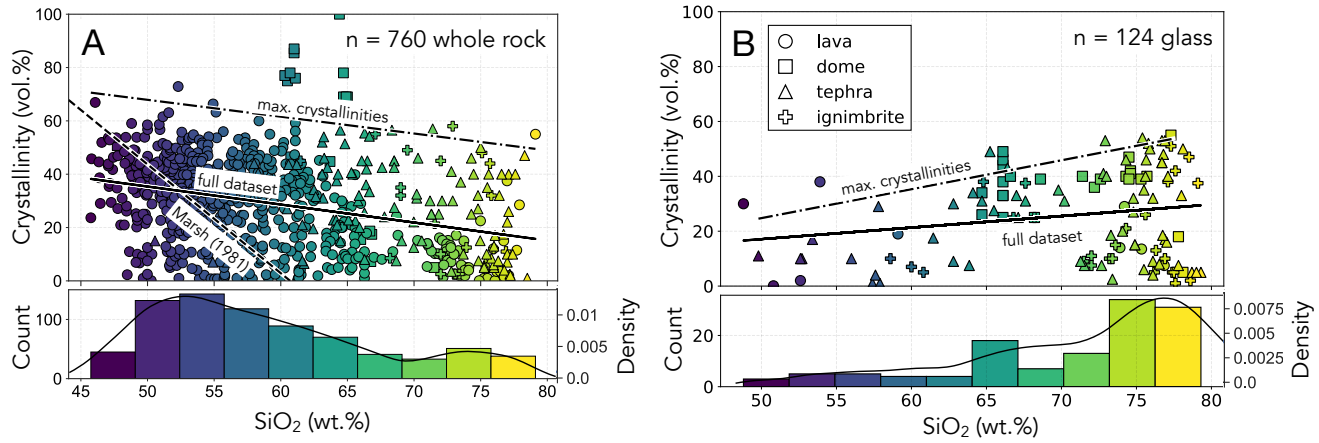

Figure 3: Crystallinity with silica content of the 884 samples with available SiO_2 data (includes Brophy [1991] compilation) grouped by whole rock [A] and glass samples [B]. The dashed line is the linear regression for Marsh [1981] lava dataset, the solid line is the linear regression for the entire dataset (i.e. 760 whole rock and 124 glass samples compiled in this study), and the dot-dash line represents the linear regression of the maximum crystallinity values for each SiO_2 bin but excluding dome samples that have high crystallinities. Symbol shapes correspond to eruptive style, in which there is only a significant correlation between SiO_2 and crystallinity of lava samples (see Supplementary Material, Figure S4). Values that accompany linear regressions can be found in Table 1. The histogram on the bottom shows the counts of data over the range of silica contents sampled (bin size = 10) and also includes a kernel density estimate (black solid line). The color scheme corresponds with SiO_2 content, where dark colors are low SiO_2, and lighter colors are high SiO_2.

(see Section 2). Results depend largely on H_2O contents as these strongly influence the resulting melt viscosity by disrupting polymerization (Figure 4A). When assuming a water content of 0.5 wt.% H_2O, 62 % of analyses have calculated effective viscosities at or below 10^6 Pa.s, the value identified by Takeuchi [2011] as the critical effective viscosity for eruption (grey dashed line: Figure 4B–D), and 70 % and 85 % have calculated effective viscosities below this for 2 and 5 wt.% H_2O, respectively. At 0.5 wt.% H_2O, the 5th and 95th percentile values for viscosity are $10^{1.0}$ and 10^{12} Pa.s, whereas at 5.0 wt.% H_2O, the 5th and 95th percentile values for effective viscosity are $10^{0.6}$ and $10^{7.0}$ Pa.s (Figure 4). Note, unrealistically high-water contents ($\ll$ 10 wt.% H_2O) are required to get all calculated effective viscosities under the 10^6 Pa.s threshold defined by Takeuchi [2011]. Our data also shows a relationship between melt viscosity and effective viscosity, where unsurpris-

ingly, increasing melt viscosity increases linearly with SiO_2 content (Figure 4A). Lastly, in general, increasing crystallinity is positively correlated with increasing effective viscosity, although not linearly.

4 Discussion

4.1 Critical crystallinity

An important outcome of this study is the examination of a critical crystallinity value (or range) for magmas where they are no longer able to erupt. If we consider our compiled dataset as representing the set of eruptible magma crystallinities, then the maximum values we observe should approximate the critical crystallinity. As stated before, the observed 95^{th} percentile crystallinities for lava, dome, tephra, and ignimbrite samples in our compilation are 50, 78, 53, and 51 vol.% (Figure 2; Table 1), and the 95^{th} percentile crystallinity for the entire dataset is 55 vol.%. Thus, with the exception of some dome eruptions (see below), results from our compilation are consistent with earlier work that suggest the maximum crystallinity for erupted magmas is 50–60 vol.% crystals [Marsh 1981; Brophy 1991; Scaillet et al. 1998; Takeuchi 2011]. In terms of different eruption styles, ignimbrite, tephra, and lava samples do not have crystallinities that exceed 60 vol.%. Thus, although there have been suggestions that eruption could occur in magmas with higher crystallinities [e.g. Bergantz et al. 2017], our results appear to empirically confirm that for the vast majority of erupted magmas, 50–60 vol.% crystals is an important limit for eruptibility across a broad range of eruption types, magma compositions, and tectonic settings.

Some dome samples appear to be an exception. Although most dome samples have crystallinities below 50–60 vol. %, there are also a significant number of erupted dome samples (~20 %) with crystallinities that exceed 60 vol.% and reach up to almost 100 vol.% (Figure 2; Table 1). This observation is consistent with other evidence that in some cases dome emplacement may occur in magmas that are near, or even subsolidus, and Marsh [1981] also suggested that emplacement of some domes might represent a different process to lavas. Evidence includes cataclastic deformation at the margins of dome walls, stick-slip extrusion patterns, and development of spines [Martel 2012; Pallister et al. 2013], and geochemical indicators of near-or subsolidus magma storage prior to eruption [Mucek et al. 2021]. Collectively, these observations and the high crystallinities recorded are consistent with different magma transport mechanisms for at least some lava dome eruptions [e.g. Pistone et al. 2017].

4.2 The relationship between silica content and crystallinity

Our data also allow us to reassess the relationship between crystallinity and SiO_2 content (both bulk and liquid) of erupted samples. Previous studies have argued for a correlation between these variables, with the critical crystallinity for eruption being lower in high silica liquids—reflecting increasing liquid polymerization. For example, the Marsh [1981] compilation of ~60 lavas, domes, and plugs from the Aleutians covered lava compositions from 46–62 wt.% SiO_2 and suggested a negative correlation with slope ~−4 between bulk SiO_2 and maximum crystallinity (dashed line: Figure 3; Table 1). This relationship was interpreted to reflect the increasing viscosity of the liquid fraction in these lavas influencing bulk viscosity and reducing the critical crystallinity for eruptions of more evolved compositions. The Brophy [1991] compilation consists of over 600 calc-alkaline lava flows and domes, focusing on subduction zone settings, and showed similar results to Marsh [1981], where crystallinity generally increases with decreasing SiO_2 content. The smaller compilations of Scaillet et al. [1998] and Takeuchi [2011] also both found a negative correlation between silica and maximum crystallinity.

As with previous studies, our larger whole rock dataset shows a significant correlation (P value less than 0.05) between bulk silica content and crystallinity with a slope of −0.7 (Figure 3A; Table 1). We see a similar slope of −0.6 but with a weaker correlation between silica and crystallinity when considering the maximum crystallinity value for binned SiO_2 contents (e.g. dot-dash line Figure 3A; Table 1). The slope of our dataset implies a change in ~20 % crystallinity over a compositional range from 45–80 wt.% SiO_2, which is considerably smaller than the ~4 vol.% crystals per 1 wt.% SiO_2 value observed by Marsh [1981] for Aleutian lavas (dashed line; Figure 3A and 3B). This discrepancy is likely due to our compilation covering a broader range of SiO_2, however, as suggested by Marsh [1981], the impact on bulk viscosity of changing SiO_2 in the liquid fraction may be greater in small subsets of samples from specific environments and locations.

While silica and crystallinity of whole rock samples show a significant correlation, glass samples show something slightly different. Silica content of glass samples and crystallinity display a weakly positive correlation with a slope of 0.4 (Figure 3B), opposite of the whole rock data (Figure 3A). Maximum crystallinity values binned by SiO_2 show a similar weak positive correlation with a similar slope. Note the smaller sample size (n = 124 glass) compared to whole rock (n = 760 whole rock) may contribute to the difference in slope values between Figure 3A and 3B. Alternatively, this relationship could be an artifact of natural processes. Generally, during crystallization, the majority of crystals that form have lower mol.% of SiO_2 when compared to the SiO_2 content in the initial liquid phase, and the SiO_2 fraction of the remaining silicate liquid therefore increases upon crystallization. Grouping both whole rock and glass samples by tephra, ignimbrite, and lava samples show linear regressions with broadly similar slopes between each other, but are unlike the slope for dome samples (Table 1; Supplementary Material, Figure S4). Note the smaller sample sizes and higher P values for tephra and ignimbrite suggest these correlations are not significant (Table 1).

4.3 Influences on effective viscosity and magma eruptibility

For samples where we have reported glass compositions, we calculated the effective viscosity using the crystallinity of a sample in conjunction with its melt viscosity, which was calculated using the reported glass composition at a given temperature and water content (see Section 2). Reported glass composition typically do not include H_2O or if they do these H_2O contents are likely to be impacted by degassing and not directly relevant to subvolcanic magma transport and stor-

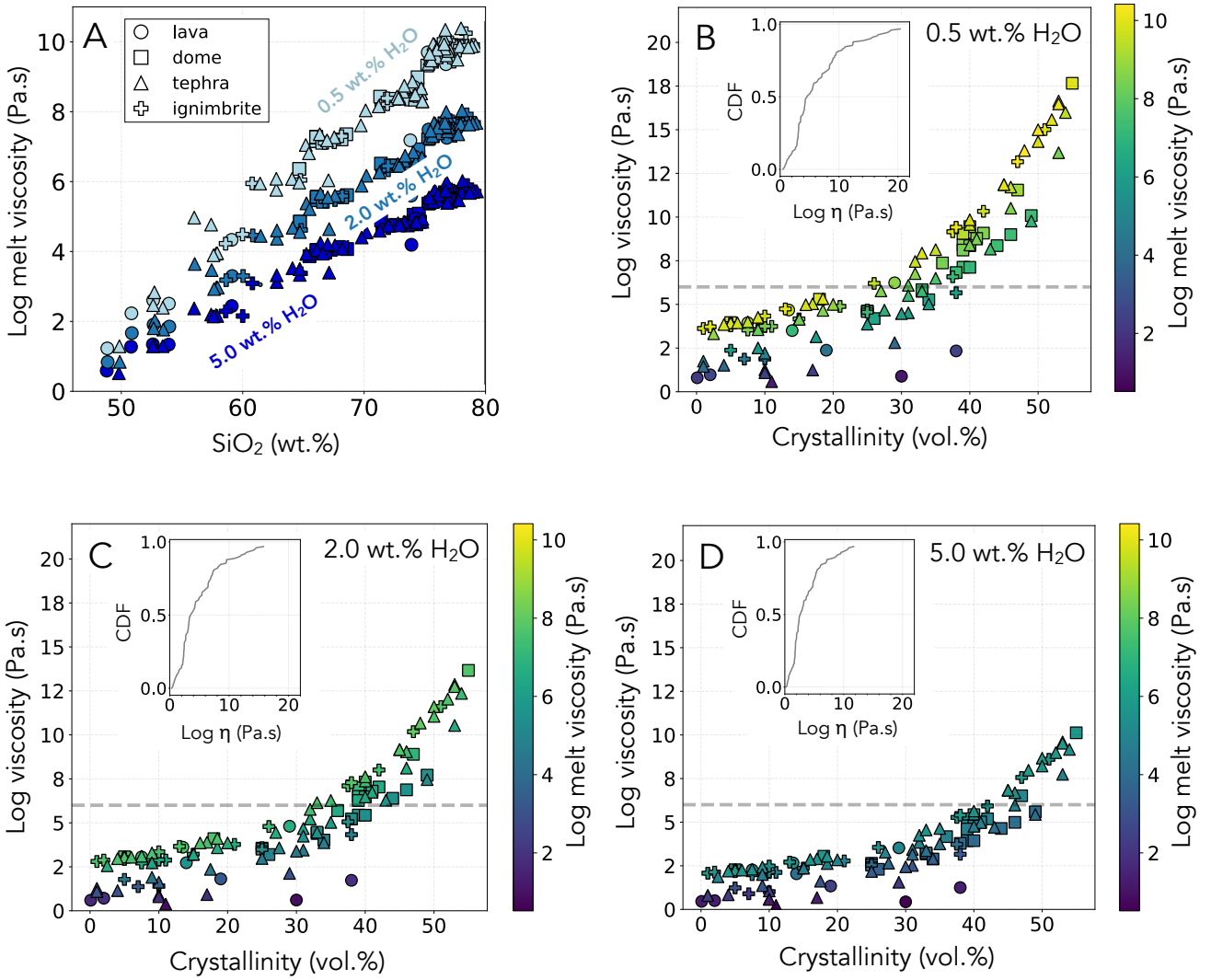

Figure 4: [A] Calculated melt viscosity values for each sample with reported major element chemistry as glass following the approach of Giordano et al. [2008] at respective temperatures assigned discretely based on relative SiO_2 content and a range of fixed water contents. Note crystal content is not considered in this calculation. Samples are also categorized by eruptive style (symbol). [B–D] Calculated effective viscosity values for each sample at variable water contents. Melt viscosity reported in [A] was used in conjunction with reported crystallinity for each sample to calculate the suspension or effective viscosity using the Maron and Pierce [1956] equation (see text). The color bar represents the melt viscosity of each sample. Dashed horizontal line is the critical viscosity of 10^6 Pa.s identified by Takeuchi [2011] for reference. A cumulative distribution function (CDF) is included as an inset.

age [e.g. Rasmussen et al. 2022]. Therefore, we calculated all compositions with representative values of H_2O contents of 0.5, 2.0, and 5.0 wt.% H_2O (Figure 4). The "critical viscosity" that marks the transition between eruptible and non-eruptible magma, was defined at 10^6 Pa.s by Takeuchi [2011] based on empirical evidence showing a restricted viscosity range between 10^4–10^6 Pa.s, suggesting more viscous magmas ($\geq 10^6$ Pa.s) cannot leave their host magma chamber and erupt (dashed line: Figure 4B–D). Most calculated effective viscosities in our study (i.e. 60 %) fall at or beneath this threshold, with the exception of very low water contents (i.e. 0.5 wt.% H_2O; Figure 4B). However, at higher crystallinities a more complex relationship exists, and comparing our calculations to a threshold of 10^6 Pa.s suggests that generally, both melt viscosity and crystallinity contribute to a magma reaching critical viscosity (Figure 4B–D).

Melt viscosity is largely dependent on SiO_2 content and H_2O content (Figure 4A), where increasing silica content of the melt increases melt viscosity and increasing water content decreases melt viscosity (Figure 4A). Both of these observations are well-established relationships [Sigurdsson et al. 2015], although a non-linear relationship between viscosity and water content has also been observed [Hess and Dingwell 1996]. Overall, our calculations suggest an important role for H_2O in controlling the melt viscosity of the silicate liquid in magmas, especially in more silica-rich liquids, as our calculated effective

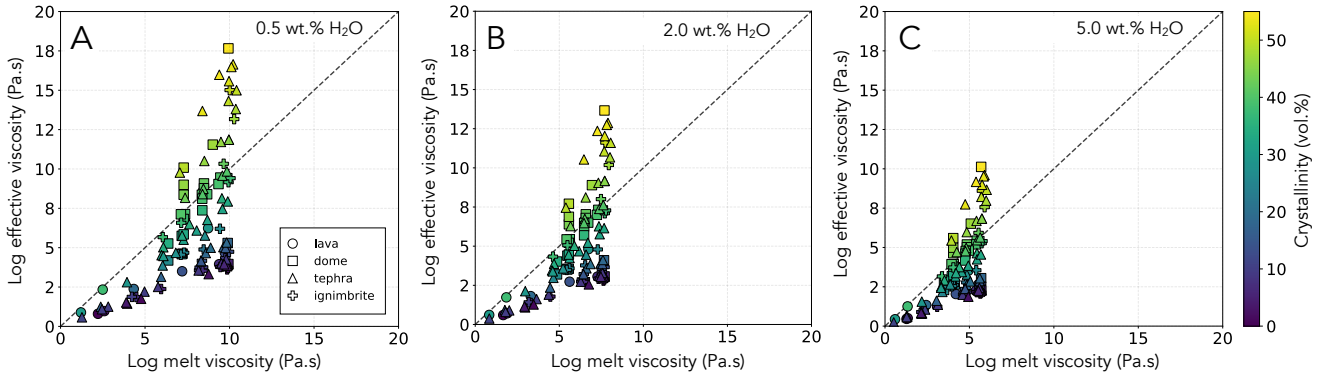

Figure 5: Calculated effective and melt viscosity values for each sample with reported major element chemistry as glass at a range of fixed water contents (see Section 2). Note crystal content is shown by the color bar and each sample is grouped by eruptive style (symbol). The dashed line represents a 1:1 line.

viscosities for lower water contents show significant proportions of samples well above the 10^6 Pa.s threshold (Figure 4B). Fewer samples (15 %) lie above this threshold for higher water content with 5.0 wt.% H_2O (Figure 4D). This is equivalent to a saturation pressure for a magma storage depth of ~4–6 km, broadly consistent with observed magma storage in the shallow crust [e.g. Huber et al. 2019; Wieser et al. 2023]. Unrealistically high-water contents ($\ll$ 10 wt.% H_2O) are required to get all calculated viscosities below the defined threshold, suggesting 10^6 Pa.s is not completely representative value that distinguishes eruptible from non-eruptible magmas, or there are other mechanisms that allow more crystal-rich magmas to erupt. The higher melt viscosities of silicic liquids also allow a magma to reach the 10^6 Pa.s threshold at lower crystal fractions (Figure 4B–D). For example, a sample with 75 wt.% SiO_2 and 5 wt.% H_2O in our dataset reaches the critical viscosity (10^6 Pa.s) at 40 vol.% crystallinity while a sample with 65 wt.% SiO_2 and 5 wt.% H_2O reaches the critical viscosity at 50 vol.% crystallinity.

Beyond melt viscosity, it is clear that crystallinity also greatly influences effective viscosity. Figure 5 shows effective and melt viscosity plotted near a 1:1 line in which crystal content is shown for each sample by the color bar. Here it is apparent that at crystallinities >40 vol.%, crystallinity is far more influential than melt viscosity. In some cases, crystal contents double the relative viscosity value (Figure 5A–C). Melt viscosity and effective viscosity approach the 1:1 line at lower crystals contents, a relationship that has been well established by previous work (e.g. review by Mader et al. [2013]). In other words, samples with crystallinities >40 vol.% reach and/or exceed critical viscosity threshold of 10^6 Pa s far more efficiently. Our compilation suggests that across the entire spectrum of erupted igneous compositions melt viscosity and crystal content both play important roles in effective viscosity. For low volume fractions of crystals, melt viscosity seems to control the effective viscosity evolution (as observed elsewhere, e.g. Pereira et al. [2022] and Zandonà et al. [2023]), while for crystallinities higher than 40 vol.% crystal fraction is the most important feature controlling effective viscosity of magmas.

5 Conclusions

Our compiled dataset of the crystallinity of volcanic rocks shows erupted rocks with crystallinities greater than 60 vol.% are very rare in nature and are largely limited to a small subset of lava dome samples. These results suggest that the widely used critical crystallinity threshold of 50–60 % crystals represent a fundamental limit for eruptibility for most magmas. Our data also highlight the important influence of liquid SiO_2 content on the critical crystallinity, with an apparent reduction in critical crystallinity of up to ~20 vol.% crystals for bulk compositions between basalt and rhyolite. However, the magnitude of this effect also appears lower in our larger compilation than in previous work based on more limited sample collections. Melt viscosity (as a function of SiO_2, temperature, and H_2O content) and crystallinity both play important roles on increasing effective viscosity, where melt viscosity plays a more important role at low crystal fractions, and crystallinity plays a more important role at crystallinities greater than ~40 vol.%.

Author Contributions

Shamloo is responsible for the project design, data compilation, modeling, calculations, and writing of this manuscript. Kent assisted with project design and writing of this manuscript.

Acknowledgements

Authors would like to thank an anonymous reviewer whose insight and expertise greatly improved this manuscript. Thank you to George Bergantz for helpful tweets and conversations. Thank you to Christy Till for inspiration of the slushy-magma-mush analogy. This work was supported by an NSF EAR Postdoctoral Fellowship [1952808] awarded to Shamloo and NSF grant [1850779] to Kent.

Data Availability

Compilation data (in form of excel file) and supplemental figures referenced in text can be found at Zenodo open-access repository: https://zenodo.org/deposit/7754305.

References

Bachmann, O. (2004). "On the Origin of Crystal-poor Rhyolites: Extracted from Batholithic Crystal Mushes". *Journal of Petrology* 45(8), pages 1565–1582. DOI: 10.1093/petrology/egh019.

Bachmann, O. and G. Bergantz (2008). "The Magma Reservoirs That Feed Supereruptions". *Elements* 4(1), pages 17–21. DOI: 10.2113/gselements.4.1.17.

Bergantz, G. W., J. M. Schleicher, and A. Burgisser (2017). "On the kinematics and dynamics of crystal-rich systems". *Journal of Geophysical Research: Solid Earth* 122(8), pages 6131–6159. DOI: 10.1002/2017jb014218.

Brophy, J. G. (1991). "Composition gaps, critical crystallinity, and fractional crystallization in orogenic (calc-alkaline) magmatic systems". *Contributions to Mineralogy and Petrology* 109(2), pages 173–182. DOI: 10.1007/bf00306477.

Caricchi, L., L. Burlini, P. Ulmer, T. Gerya, M. Vassalli, and P. Papale (2007). "Non-Newtonian rheology of crystal-bearing magmas and implications for magma ascent dynamics". *Earth and Planetary Science Letters* 264(3–4), pages 402–419. DOI: 10.1016/j.epsl.2007.09.032.

Cimarelli, C., A. Costa, S. Mueller, and H. M. Mader (2011). "Rheology of magmas with bimodal crystal size and shape distributions: Insights from analog experiments: rheology of porphyritic magmas". *Geochemistry, Geophysics, Geosystems* 12(7). DOI: 10.1029/2011gc003606.

Cooper, K. M. and A. J. R. Kent (2014). "Rapid remobilization of magmatic crystals kept in cold storage". *Nature* 506(7489), pages 480–483. DOI: 10.1038/nature12991.

Dingwell, D. B. (1996). "Volcanic Dilemma–Flow or Blow?" *Science* 273(5278), pages 1054–1055. DOI: 10.1126/science.273.5278.1054.

Einstein, A. (1906). "Eine neue Bestimmung der Moleküldimensionen". *Annalen der Physik* 324(2), pages 289–306. DOI: 10.1002/andp.19063240204.

Ewart, A. (1976). "Mineralogy and chemistry of modern orogenic lavas — some statistics and implications". *Earth and Planetary Science Letters* 31(3), pages 417–432. DOI: 10.1016/0012-821x(76)90124-2.

Giordano, D., J. K. Russell, and D. B. Dingwell (2008). "Viscosity of magmatic liquids: A model". *Earth and Planetary Science Letters* 271(1–4), pages 123–134. DOI: 10.1016/j.epsl.2008.03.038.

Gonnermann, H. M. and M. Manga (2003). "Explosive volcanism may not be an inevitable consequence of magma fragmentation". *Nature* 426(6965), pages 432–435. DOI: 10.1038/nature02138.

Hess, K. and D. B. Dingwell (1996). "Viscosities of hydrous leucogranitic melts: A non-Arrhenian model". *American Mineralogist: Journal of Earth and Planetary Materials* 81(9-10), pages 1297–1300.

Hildreth, W. (2004). "Volcanological perspectives on Long Valley, Mammoth Mountain, and Mono Craters: several contiguous but discrete systems". *Journal of Volcanology and Geothermal Research* 136(3–4), pages 169–198. DOI: 10.1016/j.jvolgeores.2004.05.019.

Huber, C., M. Townsend, W. Degruyter, and O. Bachmann (2019). "Optimal depth of subvolcanic magma chamber growth controlled by volatiles and crust rheology". *Nature Geoscience* 12(9), pages 762–768. DOI: 10.1038/s41561-019-0415-6.

Ishibashi, H. and H. Sato (2007). "Viscosity measurements of subliquidus magmas: Alkali olivine basalt from the Higashi-Matsuura district, Southwest Japan". *Journal of Volcanology and Geothermal Research* 160(3–4), pages 223–238. DOI: 10.1016/j.jvolgeores.2006.10.001.

Jaupart, C. and C. J. Allègre (1991). "Gas content, eruption rate and instabilities of eruption regime in silicic volcanoes". *Earth and Planetary Science Letters* 102(3–4), pages 413–429. DOI: 10.1016/0012-821x(91)90032-d.

Klemetti, E. W. and M. A. Clynne (2014). "Localized Rejuvenation of a Crystal Mush Recorded in Zircon Temporal and Compositional Variation at the Lassen Volcanic Center, Northern California". *PLoS ONE* 9(12). Edited by V. C. Smith, e113157. DOI: 10.1371/journal.pone.0113157.

Koleszar, A. M., A. J. Kent, P. J. Wallace, and W. E. Scott (2012). "Controls on long-term low explosivity at andesitic arc volcanoes: Insights from Mount Hood, Oregon". *Journal of Volcanology and Geothermal Research* 219–220, pages 1–14. DOI: 10.1016/j.jvolgeores.2012.01.003.

Lejeune, A.-M. and P. Richet (1995). "Rheology of crystal-bearing silicate melts: An experimental study at high viscosities". *Journal of Geophysical Research: Solid Earth* 100(B3), pages 4215–4229. DOI: 10.1029/94jb02985.

Mader, H., E. Llewellin, and S. Mueller (2013). "The rheology of two-phase magmas: A review and analysis". *Journal of Volcanology and Geothermal Research* 257, pages 135–158. DOI: 10.1016/j.jvolgeores.2013.02.014.

Manga, M., J. Castro, K. V. Cashman, and M. Loewenberg (1998). "Rheology of bubble-bearing magmas". *Journal of Volcanology and Geothermal Research* 87(1–4), pages 15–28. DOI: 10.1016/s0377-0273(98)00091-2.

Maron, S. and P. Pierce (1956). "Application of ree-eyring generalized flow theory to suspensions of spherical particles". *Journal of Colloid Science* 11(1), pages 80–95. DOI: 10.1016/0021-9797(56)90012-1.

Marsh, B. D. (1981). "On the crystallinity, probability of occurrence, and rheology of lava and magma". *Contributions to Mineralogy and Petrology* 78(1), pages 85–98. DOI: 10.1007/bf00371146.

Martel, C. (2012). "Eruption Dynamics Inferred from Microlite Crystallization Experiments: Application to Plinian and Dome-forming Eruptions of Mt. Pelee (Martinique, Lesser Antilles)". *Journal of Petrology* 53(4), pages 699–725. DOI: 10.1093/petrology/egr076.

Mucek, A. E., M. Danišík, S. L. de Silva, D. P. Miggins, A. K. Schmitt, I. Pratomo, A. Koppers, and J. Gillespie (2021). "Resurgence initiation and subsolidus eruption of cold carapace of warm magma at Toba Caldera, Sumatra". *Communications Earth & Environment* 2(1). DOI: 10.1038/s43247-021-00260-1.

Mueller, S., E. W. Llewellin, and H. M. Mader (2010). "The rheology of suspensions of solid particles". *Proceedings of the Royal Society A: Mathematical, Physical and Engineering Sciences* 466(2116), pages 1201–1228. DOI: 10.1098/rspa.2009.0445.

– (2011). "The effect of particle shape on suspension viscosity and implications for magmatic flows". *Geophysical Research Letters* 38(13). DOI: 10.1029/2011gl047167.

Mysen, B. and D. Neuville (1995). "Effect of temperature and TiO2 content on the structure of Na2Si2O5 Na2Ti2O5 melts and glasses". *Geochimica et Cosmochimica Acta* 59(2), pages 325–342. DOI: 10.1016/0016-7037(94)00290-3.

Neuville, D. R. and B. O. Mysen (1996). "Role of aluminium in the silicate network: In situ, high-temperature study of glasses and melts on the join SiO2-NaAlO2". *Geochimica et Cosmochimica Acta* 60(10), pages 1727–1737. DOI: 10.1016/0016-7037(96)00049-x.

Okumura, S., H. Ishibashi, S. Itoh, A. Suzumura, Y. Furukawa, T. Miwa, and H. Kagi (2021). "Decompression experiments for sulfur-bearing hydrous rhyolite magma: Redox evolution during magma decompression". *American Mineralogist* 106(2), pages 216–225. DOI: 10.2138/am-2020-7535.

Okumura, S., S. L. de Silva, M. Nakamura, and O. Sasaki (2019). "Caldera-forming eruptions of mushy magma modulated by feedbacks between ascent rate, gas retention/loss and bubble/crystal framework interaction". *Scientific Reports* 9(1). DOI: 10.1038/s41598-019-52272-9.

Okumura, S., K. Uesugi, A. Goto, T. Sakamaki, K. Matsumoto, A. Takeuchi, and A. Miyake (2022). "Rheology of nanocrystal-bearing andesite magma and its roles in explosive volcanism". *Communications Earth & Environment* 3(1). DOI: 10.1038/s43247-022-00573-9.

Pallister, J. S., K. V. Cashman, J. T. Hagstrum, N. M. Beeler, S. C. Moran, and R. P. Denlinger (2013). "Faulting within the Mount St. Helens conduit and implications for volcanic earthquakes". *Geological Society of America Bulletin* 125(3–4), pages 359–376. DOI: 10.1130/b30716.1.

Papale, P. (1999). "Strain-induced magma fragmentation in explosive eruptions". *Nature* 397(6718), pages 425–428. DOI: 10.1038/17109.

Pereira, L., J. Vasseur, F. B. Wadsworth, F. Trixler, and D. B. Dingwell (2022). "Interparticle and Brownian forces controlling particle aggregation and rheology of silicate melts containing platinum-group element particles". *Scientific Reports* 12(1). DOI: 10.1038/s41598-022-12948-1.

Pereira Machado, N. M., L. Pereira, M. Neyret, C. Lemaître, and P. Marchal (2022). "Influence of platinum group metal particle aggregation on the rheological behavior of a glass melt". *Journal of Nuclear Materials* 563, page 153618. DOI: 10.1016/j.jnucmat.2022.153618.

Pistone, M., A. G. Whittington, B. J. Andrews, and E. Cottrell (2017). "Crystal-rich lava dome extrusion during vesiculation: An experimental study". *Journal of Volcanology and Geothermal Research* 347, pages 1–14. DOI: 10.1016/j.jvolgeores.2017.06.018.

Popa, R.-G., O. Bachmann, and C. Huber (2021). "Explosive or effusive style of volcanic eruption determined by magma storage conditions". *Nature Geoscience* 14(10), pages 781–786. DOI: 10.1038/s41561-021-00827-9.

Rasmussen, D. J., T. A. Plank, D. C. Roman, and M. M. Zimmer (2022). "Magmatic water content controls the pre-eruptive depth of arc magmas". *Science* 375(6585), pages 1169–1172. DOI: 10.1126/science.abm5174.

Rohatgi, A. (2014). *WebPlotDigitizer user manual version 3.4*. URL: http://arohatgi.%20info/WebPlotDigitizer/app.

Roscoe, R. (1952). "The viscosity of suspensions of rigid spheres". *British Journal of Applied Physics* 3(8), pages 267–269. DOI: 10.1088/0508-3443/3/8/306.

Rubin, A. (1995). "Propagation of Magma-Filled Cracks". *Annual Review of Earth and Planetary Sciences* 23(1), pages 287–336. DOI: 10.1146/annurev.earth.23.1.287.

Ruprecht, P. and O. Bachmann (2010). "Pre-eruptive reheating during magma mixing at Quizapu volcano and the implications for the explosiveness of silicic arc volcanoes". *Geology* 38(10), pages 919–922. DOI: 10.1130/g31110.1.

Sato, H. (2005). "Viscosity measurement of subliquidus magmas: 1707 basalt of Fuji volcano". *Journal of Mineralogical and Petrological Sciences* 100(4), pages 133–142. DOI: 10.2465/jmps.100.133.

Scaillet, B., F. Holtz, and M. Pichavant (1998). "Phase equilibrium constraints on the viscosity of silicic magmas: 1. Volcanic-plutonic comparison". *Journal of Geophysical Research: Solid Earth* 103(B11), pages 27257–27266. DOI: 10.1029/98jb02469.

Sigurdsson, H., B. Houghton, S. McNutt, and J. Rymer H.and Stix, editors (2015). 2nd edition. London: Academic Press. ISBN: 9780123859389. DOI: 10.1016/c2015-0-00175-7.

Solano, J. M. S., M. D. Jackson, R. S. J. Sparks, J. D. Blundy, and C. Annen (2012). "Melt Segregation in Deep Crustal Hot Zones: a Mechanism for Chemical Differentiation, Crustal Assimilation and the Formation of Evolved Magmas". *Journal of Petrology* 53(10), pages 1999–2026. DOI: 10.1093/petrology/egs041.

Stevenson, R. J., D. B. Dingwell, N. S. Bagdassarov, and C. R. Manley (2001). "Measurement and implication of "effective" viscosity for rhyolite flow emplacement". *Bulletin of Volcanology* 63(4), pages 227–237. DOI: 10.1007/s004450100137.

Takeuchi, S. (2011). "Preeruptive magma viscosity: An important measure of magma eruptibility". *Journal of Geophysical Research* 116(B10). DOI: 10.1029/2011jb008243.

Van Zalinge, M. E., D. F. Mark, R. S. J. Sparks, M. M. Tremblay, C. B. Keller, F. J. Cooper, and A. Rust (2022). "Timescales for pluton growth, magma-chamber formation and supereruptions". *Nature* 608(7921), pages 87–92. DOI: 10.1038/s41586-022-04921-9.

Vetere, F., H. Behrens, F. Holtz, G. Vilardo, and G. Ventura (2010). "Viscosity of crystal-bearing melts and its implication for magma ascent". *Journal of Mineralogical and Petrological Sciences* 105(3), pages 151–163. DOI: 10.2465/jmps.090402.

Wieser, P. E., A. J. R. Kent, C. B. Till, and G. A. Abers (2023). "Geophysical and Geochemical Constraints on Magma Storage Depths Along the Cascade Arc: Knowns and Unknowns". *Geochemistry, Geophysics, Geosystems* 24(11). DOI: 10.1029/2023gc011025.

Zandonà, A., A. Scarani, J. Löschmann, M. R. Cicconi, F. Di Fiore, D. de Ligny, J. Deubener, A. Vona, M. Allix, and D. Di Genova (2023). "Non-stoichiometric crystal nucleation in a spodumene glass containing TiO2 as seed former: Effects on the viscosity of the residual melt". *Journal of Non-Crystalline Solids* 619, page 122563. DOI: 10.1016/j.jnoncrysol.2023.122563.